The continental subduction factory as a precursor to long-term volatile storage in continental lithospheric mantle

Bibiana Förster[1], Sonja Aulbach[2*], Gray E. Bebout[3], Gianluca Bianchini[4], Claudio Natali[4], Roberto Braga[1]

[1] Dipartimento di Scienze Biologiche, Geologiche ed Ambientali, Università di Bologna, Piazza di Porta San Donato 1, 40126 Bologna, Italy
[2] Institut für Geowissenschaften, Goethe-Universität Frankfurt, 60438 Frankfurt am Main, Germany
[3] Department of Earth and Environmental Sciences, Lehigh University, 1 West Packer Avenue, Bethlehem, PA 18015, USA
[4] Dipartimento di Fisica e Scienze della Terra, Università di Ferrara, Via Saragat 1, 44124 Ferrara, Italy

*Corresponding authors. *E-mail address*: s.aulbach@em.uni-frankfurt.de

Text S1 and Figures S1 to S6

1. Geology and prior work
2. Semi-quantitative measurement of C concentrations by multiphase carbon analyser
3. Tests to ensure reliability of isotope analyses of carbonate-poor samples and carbonate leachates
4. Isotopic modelling rationale and results
5. Additional references
6. Supplementary figures

1. Geology and prior work

Geology and samples

The Ulten Zone in the Eastern Italian Alps is a tectonic unit belonging to the Austroalpine Tonale nappe (Fig. 1). It represents a fragment of the Late Paleozoic Variscan belt (Godard et al., 1996) involved in continent-continent collision during the Variscan orogeny. Due to the weak overprint by Alpine metamorphism, the pre-Alpine evolution of the Ulten Zone is still recorded in the mineral assemblages, textures and chemical signatures of its various rock types (Godard et al., 1996; Hauzenberger et al., 1996; Martin et al., 1998). The peridotites are thought to derive from the supra-subduction zone mantle wedge, parts of which were entrained by the crustal slab (Nimis and Morten, 2000). The Ulten Zone mostly consists of garnet-kyanite paragneiss, migmatites and minor orthogneiss (Godard et al., 1996; Martin et al., 1998; Del Moro et al., 1999) and contains lenses (up to several hundred meters in length) of ultramafic rocks.

In addition to a legacy collection at Università di Bologna, comprising samples from Mount Hochwart, Lavazze Valley, Strada Stadale, Seefeldalm and Buca di Cloz, new samples occurring *in situ*, in boulders or in debris fields were collected during more recent field campaigns (Förster et al., 2017; Gudelius et al., 2019) (Table S1).

Metamorphic evolution of the ultramafic rocks and their volatile-bearing mineral inventory

The dominant variety of the Ulten Zone peridotite is a mylonitic fine-grained peridotite (0.2 mm to 1 mm grain size), often garnet- and amphibole-bearing, and occasionally with an amphibole-chlorite-bearing assemblage and pseudomorphs after garnet (Morten and Obata, 1983; Obata and Morten, 1987; Morten and Obata, 1990; Godard et al., 1996; Rampone and Morten, 2001; Tumiati et al., 2003, 2005, 2007; Scambelluri et al., 2006; Marocchi et al., 2007, 2009, 2010). The subordinate variety is represented by coarse-grained (average grain size of minerals ~0.5-1.0 cm) garnet-bearing and garnet-free peridotites (Obata and Morten, 1987). The initial degrees of partial melting experienced by the peridotites – presumably leading to the stabilisation of the continental lithospheric that ultimately became part of the Variscan subduction zone – have been estimated at 10-20% (Ionov et al., 2017). These estimates are minima, bearing in mind subsequent enrichment processes and secondary depletion of magmaphile elements related to their fluid-assisted mineralogical evolution involving garnet- and clinopyroxene-breakdown (Gudelius et al., 2019). Pyroxenite veins (mm to 10s of cm width) hosted by the peridotites display a similar evolution from coarse-grained clinopyroxenite indicative of interaction with or precipitation from mafic melts during the hot mantle wedge stage, to fine-grained garnet-amphibole pyroxenites/websterites after interaction with crustal fluids (Morten and Obata, 1983; Gudelius et al., 2019, and references therein; Pellegrino et al., 2021). In addition, phlogopite, talc, anthophyllite and tremolite occur at the contact between the peridotite lenses and the crustal gneisses, exemplified by the Mt. Hochwart locality (Marocchi et al., 2009).

Previous studies report the presence of dolomite, magnesite and calcite in the Ulten Zone peridotites (Obata and Morten, 1987; Godard et al., 1996; Morten and Trommsdorff, 2003; Tumiati et al., 2005; Braga and Sapienza, 2007; Marocchi et al., 2007; Sapienza et al., 2009; Malaspina and Tumiati, 2012; Förster et al., 2017; Gudelius et al., 2019; Consuma et al., 2020), while sulphide and its sulphur isotopic composition in combination with the $^{87}Sr/^{86}Sr$ of carbonates and amphiboles was the focus of Consuma et al. (2021) who also summarised the evolution of the volatile-bearing mineral inventory.

Based on these prior works, a four-stage metamorphic evolution during Variscan collision and post-collisional exhumation is recognised, for which conventional geothermobarometry, consideration of phase stabilities and geodynamic modelling have allowed pressure-temperature estimates to be made (Nimis and Morten, 2000; Braga and Sapienza, 2007; Förster et al., 2017; Consuma et al., 2020), while geochronological (Tumiati et al., 2003, and references therein) and numerical modelling constraints (Ranalli et al., 2005) provide a timeline:

(1) Residence of pre-Variscan lithospheric mantle in the hot mantle wedge. H_2S-CO_2-bearing silicate melts infiltrated the peridotites when they still resided in the hot mantle wedge. This stage is represented by coarse-grained protogranular peridotites consisting of olivine, enstatite, diopside and Cr-Al spinel and recorded by grains of dolomite (and calcite-brucite symplectites after dolomite) as inclusions in primary Al-Cr-spinel, whereas no primary carbonates occur in the matrix. Sulphur in matrix pentlandite in the pyroxenites is isotopically heavy. The pressure-temperature conditions for this stage have been estimated at 1.3-1.6 GPa and 1200 °C, respectively.

(2) High-pressure eclogite-facies re-equilibration at 330 Ma. Part of the mantle wedge was down-dragged with the subducting slab, leading to eclogite-facies metamorphism and growth of coronitic garnet. This was accompanied by metasomatism by aqueous fluids with intermediate CO_2/H_2O, which were released by the subducting continental slab, and is evidenced by growth of amphibole (3-18 vol.%, locally exceeding 20 vol.%), apatite and of interstitial matrix dolomite ± magnesite, and by LILE- and LREE-enrichment in whole rocks and minerals. Interstitial dolomite grains are often spatially associated with other metasomatic phases, such as amphibole and apatite, and occasionally included in garnet. Elevated sulphide $\delta^{34}S$ (up to +3.43 ‰) and carbonate $^{87}Sr/^{86}Sr$ (>0.7052) support formation from or interaction with an isotopically heavy crustal fluid. The pressure-temperature conditions for this stage have been estimated at 2.2-2.7 GPa and ~850 °C, respectively.

(3) Early fast exhumation and chloritisation (~330-300 Ma). During the retrograde path of the peridotites, aqueous fluids with high CO_2/H_2O caused the formation of chlorite and of multiple carbonate generations, including coexisting dolomite and magnesite, as observed in a coarse-grained garnet-free peridotite, in anhedral dolomite and distinct dolomite veins that crosscut the matrix of fine-grained peridotites, and in retrograde magnesite associated with dolomite. The isotopic composition of the fluid varied strongly, probably as a function of the degree of interaction with the mantle, with dolomite $^{87}Sr/^{86}Sr$ of 0.7036-0.7083 and pentlandite with $\delta^{34}S$ of -0.38‰ to +0.60 ‰. The pressure-temperature conditions for this stage have been estimated at 1.0-2.2 GPa and ~650-700 °C, respectively.

(4) Late slow exhumation and serpentinisation (~300-200 Ma). Peridotite interaction with serpentinising fluids having low CO_2/H_2O led to precipitation of serpentine and dolomite breakdown, resulting in the transformation of dolomite into symplectites of calcite + brucite and the liberation of carbon to the fluid, according to the reaction $CaMg(CO_3)_2 + H_2O = CaCO_3 + Mg(OH)_2 + CO_2$. Infiltration of fluids with high $a(CO_2)$ led to local formation of carbonate veins, mainly calcite, in pre-existing pathways and/or co-crystallising with serpentine, but texturally late dolomite veins with high $^{87}Sr/^{86}Sr$ (0.711) are also observed. Pentlandite has highly variable $\delta^{34}S$ of -0.29‰ to +3.76 ‰, but the appearance of sulphur-poor and nickel-rich sulphides (millerite, heazlewoodite) points to desulphurisation during this stage, during which ^{32}S may have been preferentially lost. The pressure-temperature conditions for this stage have been estimated at <1.0 GPa and <600 °C, respectively.

In addition to the collection of ultramafic samples described in the main text, four samples representative of the Ulten Zone crust were selected for study, comprising a garnet-staurolite gneiss (TUN3), a garnet-kyanite gneiss (NB14; Bargossi et al., 2003) and two stromatic migmatites (NB2 and NB11; Braga and Massonne, 2008; 2012).

Oxygen fugacity estimates

The speciation of volatiles and the stability of volatile-bearing minerals strongly depends on fO_2. At the *P* range estimated for Ulten Zone garnet-bearing peridotites (~2-3 GPa), and based on $Fe^{3+}/\Sigma Fe$ in garnet (<0.05), fO_2 (expressed relative to the Fayalite-Magnetite-Quartz buffer FMQ) ranges from FMQ-2.4 to FMQ-0.32. These low oxygen fugacities are only just permissive of the presence of oxidised carbon as stored in the carbonates if a low *P* of 2.0-2.5 GPa is assumed (Gudelius et al. 2019) (Fig. 1c). Higher garnet $Fe^{3+}/\Sigma Fe$ (up to 0.14) and fO_2 (up to FMQ+2) were reported by Malaspina et al. (2009). Malaspina et al. (2009) find correlations between fO_2 and the presence of amphibole plus dolomite, perhaps reflecting ingress of CO_2-bearing aqueous fluids. Since $Fe^{3+}/\Sigma Fe$ in both studies was determined using the same method, this may reflect real geological variability, consistent with the recognised fO_2 heterogeneity in the subduction environment (Cannaò and Malaspina, 2018).

Geochemical and isotopic provinciality

Intriguingly, peridotites derived from different lenses (Samerbergalm in the NE domain vs. Seefeldalm/Malga Masa Murada in the central domain) show a striking provinciality (outlined in Fig. 1a) with respect to textures and compositions (Gudelius et al. 2019, 2022). The strongest fluid imprint, in the central domain, is expressed by high LILE contents, HREE loss due to garnet-breakdown, addition of Zr-Hf-Li, enriched Nd-Hf isotope compositions and kinetically fractionated Li isotope composition (Gudelius et al. 2019, 2022), thus documenting mobility of "canonically" fluid-immobile elements (HFSE, REE), which was tentatively ascribed to the action of halogens. The observed provinciality may point to the involvement of different metasomatic agents or to the evolution, via intense fluid-rock interactions, of a single agent. If so, it may reflect different positions of the peridotite lenses relative to the subducted slab and therefore to the crustal fluid source (Gudelius et al., 2019, 2022).

2. Semiquantitative measurement of C concentrations by multiphase carbon determinator (LECO)

A preliminary, semi-quantitative characterisation of the C concentrations in whole-rocks was carried out at Goethe University Frankfurt (Germany) using a LECO RC-412 Multiphase Carbon Determinator. Fifty-one selected whole-rock samples comprising 16 coarse-type peridotites, 13 fine-grained garnet-bearing peridotites, 20 fine-grained garnet-free peridotites and 2 amphibolitised pyroxenite samples were analysed. A calcite standard was used for calibration of the instrument. For each analysis, 0.3 g of whole-rock powder was inserted into the furnace inside a quartz container. The total C concentration was determined from the analysis of the emitted CO_2 via infrared spectrometry, after combustion of the powder in the presence of O_2. The heating was ramped up first to 550°C to largely burn the organic carbon fraction, and then up to 1000°C in order to largely burn the inorganic carbon fraction. We

note here that the speciation of the reduced carbon in the samples is unknown, and that multiple carbonate minerals may be present in a given sample. Moreover, graphitic C, if present, need not have been quantitatively burnt by 550 °C and may have contributed to the fraction produced at 1000 °C, while some carbonates, such as magnesite, may already decompose at low temperatures and may have contributed to the fraction produced at 550 °C, especially at low sample weights (Pillot et al., 2014). Results, including petrographic type, are reported in Table S4.

3. Tests to ensure reliability of isotope analyses of carbonate-poor samples and carbonate leachates

Bulk-rock total carbon concentrations and isotopic compositions

The low concentration of carbon in peridotites required detailed testing of the reliability of the analytical results. The application of this technique to study the carbon concentration and carbon isotopic composition in low-carbon matrices, such as peridotites, was previously described in Bianchini and Natali (2017). Reproducibility of three standards (Carrara marble, Jacupiranga carbonatite, and sulfanilamide) with progressively reduced sample mass allowed defining a reliability threshold of the signal at 0.90 nA for Ulten Zone peridotites (Fig. S1a). The reproducibility of the instrumental technique was tested by analysing duplicates (Fig. S1b) and the maximum variation $\Delta^{13}C$ for duplicates is 0.54‰. The measured isotopic ratios ($\delta^{13}C_m$) for the three standards conform to the theoretical ratios ($\delta^{13}C_t$; Fig. S1c). The data for the Ulten Zone peridotites plot on this curve, showing that the analytical technique is suitable for these rocks. The carbon elemental concentration is reported in wt. % and the carbon isotopic composition is notated as $\delta^{13}C$, expressing the ‰ deviation from Pee Dee Belemnite (i.e. VPDB). Results, including petrographic type, are reported in Table S5.

Carbonate dissolution testing

We conducted the testing on three representative peridotite samples (PRE-A, SBA4, WG2) with known carbonate contents based on the petrographic observations presented in Förster et al. (2017). During the testing, we increased stepwise the weight of bulk-rock powder of each sample and compared the results of the yield (amplitude divided by the weight of the powder) and the C and O isotopic composition. Based on previously reported reaction times for carbonate dissolution in phosphoric acid (Das Sharma et al., 2002; Collins et al., 2015), sample PRE-A, which contains calcite veins, reacted for 1 hour, whereas samples SBA4 containing dolomite and sample WG2 containing calcite and dolomite reacted for 3 hours. The testing aimed to obtain a threshold for the stable yield and stable isotopic ratios over a range of various sample weights. When yield and isotopic ratios remain unaffected by any further increase of the sample weight, the sample amount in this range is deemed to produce reliable results of the carbonate stable isotopic composition. For sample PRE-A, in the weight range from 5 mg to 35 mg, the yield and the C isotope ratio increase (Fig. S2a), whereas both reach stability in the range from 40 to 60 mg (standard deviation for stable-isotope ratios <0.2‰; Fig. S2b). This means that, in the range from 40 mg to 60 mg, the stable isotope analyses are the most reliable. The test results for sample SBA4 show that yield and stable-isotope ratios are stable in the sample-weight range between 80 mg and 110 mg (standard deviation for $\delta^{13}C$ and $\delta^{18}O$ ≤0.2‰; Fig. S2c,d). Slightly increasing yields and isotopic ratios, $\delta^{13}C$ from -11.3‰ to -10.4‰ and $\delta^{18}O$ from +14.5‰ to 15.7‰, over the entire range of sample weights (15 mg to 85 mg) were observed also during the testing using sample WG2 (standard deviation for $\delta^{13}C$ and $\delta^{18}O$ ~0.3‰; Fig. S2e,f). Based on the test results, ~80 mg

whole-rock powder was chosen for the analyses of the UZ peridotites, but sample weights were adjusted depending on whether initial analyses yielded suboptimal intensities. Thus, the used sample weights for the measurements range from 16 mg to 122 mg.

For sample WG2, an additional test run was carried out with 52 mg of sample and a reaction time of 30 hours in order to test possible variations of the yield and isotopic ratios after a longer reaction time. Interestingly, this run resulted in an elevated yield relative to those after 3 hours reaction time and a slightly elevated (from 0.2‰ to 1.4 ‰) O isotope ratio. This may indicate that the sample contains Mg-rich dolomite for which the reaction time with the acid is longer. This result prompted further testing designed to define the reaction time for the variable carbonate contents in the UZ peridotites with phosphoric acid (Fig. S3). The tests were carried out on samples with unknown (Fig. S3a,c,e) and multiple carbonate contents (samples containing calcite-brucite intergrowths, Fig. S3b,d,f), and reaction times were 1 hour, 3, 6 and 30 hours. For most of the tested samples, the highest absolute yield (intensity per unit of whole-rock powder, mV/mg) is obtained after 30 hours reaction (Fig. S3a,b), including significant changes in C-isotope values for some of the samples (up to 3‰, sample MZS1-6; Fig. S3c). In other cases, these values do not differ significantly for the different reaction times. In contrast, the O isotopic ratios may show significant variations (Fig. S3e,f). Thus, for whole-rock samples containing multiple carbonate phases and for samples with unknown carbonate content reaction time of 30 hours are considered the most reliable.

4. Isotopic modelling rationale and results

Fractionation factors for the isotopic modelling were retrieved from https://alphadelta.ggl.ulaval.ca. The carbonate minerals to consider are dolomite, magnesite and calcite, whereas aragonite is not expected to be stable at the *P-T* conditions recorded by Ulten Zone peridotites (Fig. 1b). The C isotopic fractionation between carbonates and CO_2 in the fluid (1000 lnα ($^{13}C/^{12}C$) or Δ(carbonate-CO_2)) does not change monotonically as a function of temperature, but is characterised by a change in sign of slope around 500 °C, such that at higher temperatures calcite is always isotopically lighter than CO_2 in the fluid, whereas dolomite and magnesite are always heavier, and show minimal inter-mineral C isotopic fractionation (Chacko et al., 1991; Scheele and Hoefs, 1992; Hoefs, 2009). With respect to oxygen, the fluid is always isotopically heavier than carbonate (Chacko et al., 1991; Zheng, 1999). The modelling only informs on the isotopic and carbon abundance trends that result from Rayleigh distillation-type processes, but the measured isotopic and compositional systematics additionally reflect the superposition of the presence of multiple generations of carbonate in some measured bulk rocks, the likelihood of variable fluid sources, and possible (partial) equilibration of the fluid with rocks of isotopic composition distinct from that of the fluid source. Results for the modelling at the conditions described below are summarised in Table S7 and displayed in Figures 3 and 4.

Equilibrium C-O isotope fractionation – the fluid at Mount Hochwart

The sample from Mount Hochwart, at the gneiss-peridotite interface, contains reaction zones recording interaction with a crustal fluid at 660-700 °C (Tumiati et al., 2007; Marocchi et al., 2009, 2010). It contains dolomite, multiple analyses of which form a sub-vertical array in $\delta^{18}O$-$\delta^{13}C$ space (Fig. 3a) that may reflect the compositional evolution of a fluid, the $\delta^{13}C$ of which overwhelmed the initially virtually carbon-free residual peridotite, as carbon is incompatible. Conversely, the fluid was, initially at low-fluid-rock ratios, itself overwhelmed

by the mantle $\delta^{18}O$ of the peridotite, and the highest $\delta^{18}O$ in dolomite from Mount Hochwart is taken to reflect a more fluid-dominated isotopic signature. The $\delta^{13}C$ of the fluid can be estimated from that of the dolomite (−10.0‰ ± 0.2‰ 1σ; n = 11; Table S5) using the calibration of Golyshev et al. (1981; calibrated for 0-1000 °C) to derive the Δ(dolomite-CO_2), which is +0.6‰ to +0.8‰ for 660-700 °C. The $\delta^{18}O$ of the fluid in equilibrium with the isotopically heaviest dolomite ($\delta^{18}O$ of +10.4‰) would be ~+5.3‰, for a Δ(dolomite-CO_2) of −5.0‰ to −5.2‰ for 660-700 °C (calibration of Zheng, 1999; for 0-1200 °C).

Rayleigh distillation modelling of rock C-$\delta^{13}C$: Carbonation during early metamorphic stages

The high-*P* Stage 2 at ~850 °C (Fig. 1b) and early exhumation (chloritisation) at 650-700 °C were characterised by dolomite addition (Fig. 1c). We model the isotopic evolution of the fluid from which dolomite precipitated at 800 and 600 °C as examples, and assume for simplicity that dolomite is the only C-bearing phase in the rock, as magnesite is a subordinate carbonate mineral in peridotites representing this stage. Equilibrium Δ(dolomite-CO_2) at these temperatures is +1.2‰ and +0.3‰, respectively. The initial total C concentration is estimated to be ~0.04 wt.%, which is roughly the concentration, at which various suggested trends in the diagram of bulk C concentration vs. $\delta^{13}C$ originate (Fig. 4a). The corresponding starting $\delta^{13}C$ at the origin is ~−12‰, which is more negative than the estimate for the fluid at Mt. Hochwart, but it is plausible that the metasomatic fluids interacting with the mantle wedge had varying crustal sources with a range of isotopic compositions. At carbon exhaustion, the fluid is taken to be capable of precipitating 2 or 0.5 wt.% of carbon as dolomite. The highest total C concentration in the measured bulk rocks is 0.3 wt.%, which is consequently achieved before the C fraction in the fluid reaches 0.2 and 0.6, respectively. The attendant change in dolomite $\delta^{13}C$ via Rayleigh distillation is <1.1‰ at all modelled conditions, thus explaining the subvertical trend dominantly for peridotites from the NE domain, i.e. increasing C content without a systematic change in $\delta^{13}C$ (Fig. 4a). The spread in bulk-rock $\delta^{13}C$ values of nearly 6‰ may reflect variable fluid $\delta^{13}C$ as a function of degree of equilibration with and/or the presence in the assemblage of ^{13}C-depleted components, as also indicated by a comparison of measured bulk rock vs. carbonate $\delta^{13}C$ (Fig. 4b).

Rayleigh distillation modelling of rock C-$\delta^{13}C$: Carbonation during exhumation

Temperatures of <600 °C have been estimated for the late exhumation stage (serpentinisation), as reviewed above, which is dominantly represented by peridotites from the SW Ulten Zone. In turn, these samples are dominated by calcite, which has on average heavier measured $\delta^{13}C$ (−7.9‰) and $\delta^{18}O$ (+17.2‰) than dolomite (−10.1‰ and +10.9‰, respectively) (Table S6). Equilibrium Δ(calcite-CO_2) at 500 and 400°C is virtually identical at −3.9‰ (calibration of Scheele and Hoefs, 1992; for 500-1200 °C). As for dolomite fractionation, we assume initial $\delta^{13}C$ of −12‰ and carbon concentration of 0.04 wt.%. The highest total C concentration in the measured bulk rocks representing the "Stage 3-4" trend in Figure 4a is only 0.1 wt.%, while the spread in bulk-rock $\delta^{13}C$ between 0.04 and 0.1 wt.% C is ~6‰ to 8‰. At the modelled conditions, these systematics can be approximated when 80% of a fluid capable of precipitating 0.1 wt.% C as calcite is consumed. The modelled trend roughly reproduces that displayed by a subgroup of samples, dominantly from the SW Ulten Zone domain, which show moderately increasing C concentration at strongly increasing $\delta^{13}C$ (Fig. 4a). Conversely, a fluid capable of precipitating a greater mass of calcite would

316 experience too little isotopic fractionation before the observed bulk-rock C concentration is
317 reached. Any fraction of a ^{13}C-depleted component in the bulk rock, as gauged in Figure 5a,
318 would imply a higher fraction of C that must be consumed via calcite fractionation in order to
319 reproduce the highest $\delta^{13}C$, while the total C precipitated must be lower. These results suggest
320 interaction with a fluid having low CO_2/H_2O that was nearly quantitatively consumed and
321 may be represented by late calcite (and magnesite) veins.
322

323 ***Rayleigh distillation modelling of rock C-$\delta^{13}C$: Dedolomitisation during exhumation***

324 Decarbonation occurred during exhumation, which is probably characterised by a continuing
325 decline of temperatures, and <600 °C has been estimated for late-stage serpentinisation, as
326 reviewed above. Dedolomitisation is manifested in the presence of calcite-brucite
327 intergrowths (Förster et al., 2017), and late-injected calcite veins may at least in part reflect
328 the crystallisation products. This metamorphic stage is dominantly represented by peridotites
329 from the SW Ulten Zone domain. We model the effect of devolatilisation at 500 and 400 °C
330 on dolomite, which persisted through Stage 3 (chloritisation) but largely disappeared at Stage
331 4 (serpentinisation). At these temperatures, the sign of CO_2-dolomite fractionation is opposite
332 that modelled above at higher temperatures, i.e. the fluid is moderately isotopically heavier
333 than coexisting dolomite, with equilibrium Δ(dolomite-CO_2) 500 and 400 °C of −0.3‰ and
334 −0.8‰, respectively (calibration of Golyshev et al., 1981). Moreover, we take into account
335 the greater fraction of a ^{13}C-depleted component in peridotites from the SW domain (Fig. 5a)
336 and also model the residue as a mixture of 90% inorganic and 10% organic carbon (with $\delta^{13}C$
337 of -27), following the modelling in Bouilhol et al. (2022). This corresponds to the median
338 ratio estimated from the difference between measured carbonate and bulk-rock $\delta^{13}C$ (as
339 discussed in the main text). The starting C concentration is taken to be 0.1 wt.% (i.e.
340 corresponding to a rock that has been mildly enriched in C), while $\delta^{13}C$ is taken to be −10‰
341 (i.e. similar to some apparently enriched peridotites) (Fig. 4a). At both temperatures the
342 modelled decrease in both C concentration and $\delta^{13}C$ provides a reasonable match for most of
343 the samples forming the "Late Stage" trend indicated in Figure 4a, of which the more
344 isotopically depleted samples have C concentrations of 0.02-0.03 wt.%. The late-stage
345 decarbonation may reflect infiltration of H_2O-rich, CO_2-poor fluids sourced from adjacent
346 metapelites, as suggested for the devolatilisation of carbonate-bearing metasediments in the
347 Italian Alps, which reflect the interplay between Rayleigh distillation and open-system
348 flushing by external fluids (Cook-Kollars et al., 2014).
349

350 ***Rayleigh distillation modelling of carbonate $\delta^{18}O$-$\delta^{13}C$***

351 The carbonate $\delta^{18}O$-$\delta^{13}C$ systematics in Figure 3, with a rough positive trend when the entire
352 dataset is considered, may reflect precipitation from an isotopically heavy (e.g., sediment-
353 equilibrated) fluid at the high end, whereas the lower values reflect peridotite having typical
354 mantle-$\delta^{18}O$ (~+5‰ to +6‰), yet very low $\delta^{13}C$. It is significant that the isotopically heavy
355 end is dominated by peridotites from the SW Ulten Zone domain, which have been overall
356 more strongly affected by exhumation-related chloritisation and serpentinisation and injection
357 of late-stage calcite veins. As outlined in the prior section, the evolution of the bulk rock to
358 heavier $\delta^{13}C$ along with a modest increase in C concentration may reflect addition of calcites
359 from a CO_2-poor fluid that was nearly consumed. Dedolomitisation at 500 or 400 °C will
360 generate a fluid the $\delta^{13}C$ of which is heavier by +0.3‰ and +0.8‰, respectively, than
361 dolomite (calibration of Golyshev et al., 1981), as noted in the prior section. With respect to

$\delta^{18}O$, we assume that the rate at which O is depleted by carbonate breakdown (gauged as the fraction F(O)) is linked to the depletion of C (F(C)) as 0.4 x F(O) +0.6. This is designed to account for the fact that silicates remain the dominant O reservoir, even after complete devolatilisation (Valley, 1986). Consequently, as noted by Collins et al. (2015), this modelling can only indicate the general topology of the modelled curve, as in detail, the total change in $\delta^{13}C$ and $\delta^{18}O$, and the exact trajectory, depend on the fraction of C and O actually devolatilised and on the modal abundances carbonate and silicate phases. At the modelled conditions, dedolomitisation at 500 or 400 °C will generate a fluid that is heavier by +6.5‰ and +7.5‰, respectively, than dolomite (calibration of Zheng, 1999). The starting $\delta^{13}C$ and $\delta^{18}O$ are taken to be −8 and +14 ‰, respectively, similar to isotopically heaviest dolomite in the sample set. The inset in Figure 3a shows that at 400 °C, the C-O isotopic trend for discrete matrix dolomite is well captured. If the isotopically heavier fluid generated by initial dedolomitisation was captured proximally and completely consumed via formation of carbonate veins, then the isotopic composition of calcite in the veins might reflect that of the fluid. Alternatively, and perhaps more likely, the isotopically heavy calcite in Figure 3a as well as the overall heavy isotopic signatures in carbonates from the SW Ulten Zone domain reflect influx of an external fluid that inherited distinct, heavier isotopic compositions from the sedimentary source.

Rayleigh distillation modelling: Decarbonation of (meta)sediments

Metasediments in the Italian Alps are characterised by carbonates largely retaining $\delta^{13}C$ of marine carbonates ($\delta^{13}C$ ~0‰), with lower values produced by a combination of decarbonation and isotopic exchange with graphite during prograde subduction (Cook-Collars et al., 2014). Similarly, the host gneisses of the Ulten Zone peridotites may have acquired their extremely low $\delta^{13}C$ (~−33‰ to −25 ‰) via a combination of processes, with final C concentrations between 0.05 and 0.22 wt.% (Table S5). Their C concentration at peak metamorphic conditions and crustal melting, as well as during subsequent exhumation, when crustal fluids are inferred to have metasomatised the embedded Ulten Zone mantle slices, is unknown. As noted above, equilibrium Δ(calcite-CO_2) at 500 and 400°C is virtually identical at −3.9‰ (calibration of Scheele and Hoefs, 1992; for 500-1200 °C). Modelling shows that for a starting concentration of 5 or 2 wt.% total C and $\delta^{13}C$ of 0‰ (similar to marine carbonate), a difference in $\delta^{13}C$ of only ~9‰ is achieved when the residue has ≤0.5 wt.% C and 90% of the initial C is devolatilised. The lower measured $\delta^{13}C$ in the Ulten Zone gneisses therefore may in part reflect the presence of reduced and isotopically light carbon. For example, all other things being equal, presence of 10% of graphite with a $\delta^{13}C$ of −27‰ will produce a residue having a $\delta^{13}C$ of -19‰. Yet lower bulk $\delta^{13}C$ determined for the gneisses may require a starting $\delta^{13}C$ that was lower than that of marine carbonates due to equilibration with graphite facilitated at near-peak temperatures (e.g. Cook-Kollars et al., 2014).

5. Additional references

Bargossi, G.M., Bondi, M., Mordenti, A., Morten, L., 2003. The abundances of 55 elements and petrovolumetric models of the crust in the Non and Ulten Valley (Site 3), in: Sassi, F.P. (Ed.), The abundance of 55 elements and petrovolumetric models of the crust in 9 type areas from the crystalline basements of Italy, with some geophysical and petrophysical data. Accademia Nazionale delle Scienze, Detta dei XL, Scritti e Documenti, Roma, pp. 163-196.

Bouilhol, P., Debret, B., Inglis, E.C., Warembourg, M., Grocolas, T., Rigaudier, T., Villeneuve, J., Burton, K.W., 2022. Decoupling of inorganic and organic carbon during slab mantle devolatilisation. Nature Communications 13, 308.

Braga, R., Massonne, H.J., 2008. Mineralogy of inclusions in zircon from high-pressure crustal rocks from the Ulten Zone, Italian Alps. Periodico Di Mineralogia 77, 43-64.

Braga, R., Massonne, H.J., 2012. H2O content of deep-seated orogenic continental crust: the Ulten Zone, Italian Alps. International Geology Review 54, 633-641.

Braga, R., Sapienza, G.T., 2007. The retrograde evolution of a dolomite-bearing hydrous peridotite from the Ulten Zone (Italian Alps). GeoActa 6, 37-45.

Cannaò, E., Malaspina, N., 2018. From oceanic to continental subduction: Implications for the geochemical and redox evolution of the supra-subduction mantle. Geosphere 14, 2311-2336.

Chacko, T., Mayeda, T.K., Clayton, R.N., Goldsmith, J.R., 1991. Oxygen and carbon isotope fractionations between CO_2 and calcite. Geochimica et Cosmochimica Acta 55, 2867-2882.

Deines, P., 2002. The carbon isotope geochemistry of mantle xenoliths. Earth-Science Reviews 58, 247-278.

Del Moro, A., Martin, S., Prosser, G., 1999. Migmatites of the Ulten Zone (NE Italy), a Record of Melt Transfer in Deep Crust. Journal of Petrology 40, 1803-1826.

Golyshev, S.I., Padalko, N.L., Pechenkin, S.A., 1981. Fractionation of stable oxygen and carbon isotopes in carbonate systems. Geochemistry International 18, 85-99.

Marocchi, M., Hermann, J., Morten, L., 2007. Evidence for multi-stage metasomatism of chlorite-amphibole peridotites (Ulten Zone, Italy): Constraints from trace element compositions of hydrous phases. Lithos 99, 85-104.

Marocchi, M., Hermann, J., Tropper, P., Bargossi, G.M., Mair, V., 2010. Amphibole and phlogopite in "hybrid" metasomatic bands monitor trace element transfer at the interface between felsic and ultramafic rocks (Eastern Alps, Italy). Lithos 117, 135-148.

Morten, L., Obata, M., 1983. Possible high-temperature origin of pyroxenite lenses within garnet peridotite, northern Italy. Bulletin de Mineralogie 106-6, 775-780.

Morten, L., Trommsdorff, V., 2003. Metamorphism and textures of dry and hydrous garnet peridotites, in: Carswell, D.A., Compagnoni, R. (Eds.), Ultrahigh pressure metamorphism. Eötvös University Press, Budapest, pp. 443-466.

Obata, M., Morten, L., 1987. Transformation of Spinel Lherzolite to Garnet Lherzolite in Ultramafic Lenses of the Austridic Crystalline Complex, Northern Italy. Journal of Petrology 28, 599-623.

Pellegrino, L., Menegon, L., Zanchetta, S., Langenhorst, F., Pollok, K., Tumiati, S., Malaspina, N., 2021. Reaction-Induced Mantle Weakening at High-Pressure Conditions: An Example From Garnet Pyroxenites of Ulten Zone (Eastern Alps, N Italy). Journal of Geophysical Research: Solid Earth 126, e2021JB022584.

Pillot, D., Deville, E., Prinzhofer, A., 2014. Identification and Quantification of Carbonate Species Using Rock-Eval Pyrolysis. Oil & Gas Science and Technology – Rev. IFP Energies nouvelles 69, 341-349.

Scheele, N., Hoefs, J., 1992. Carbon isotope fractionation between calcite, graphite and CO_2: an experimental study. Contributions to Mineralogy and Petrology 112, 35-45.

Sharma, S.D., Patil, D.J., Gopalan, K., 2002. Temperature dependence of oxygen isotope fractionation of CO2 from magnesite-phosphoric acid reaction. Geochimica et Cosmochimica Acta 66, 589-593.

Tumiati, S., Godard, G., Martin, S., Nimis, P., Mair, V., Boyer, B., 2005. Dissakisite-(La) from the Ulten zone peridotite (Italian Eastern Alps): A new end-member of the epidote group. American Mineralogist 90, 1177-1185.

Valley, J.W., 1986. Stable isotope geochemistry of metamorphic rocks. Reviews in Mineralogy and Geochemistry 16, 445-489.

Zheng, Y.-F., 1999. Oxygen isotope fractionation in carbonate and sulfate minerals. Geochemical Journal 33, 109-126.

457

458 **6. Supplementary Figures**

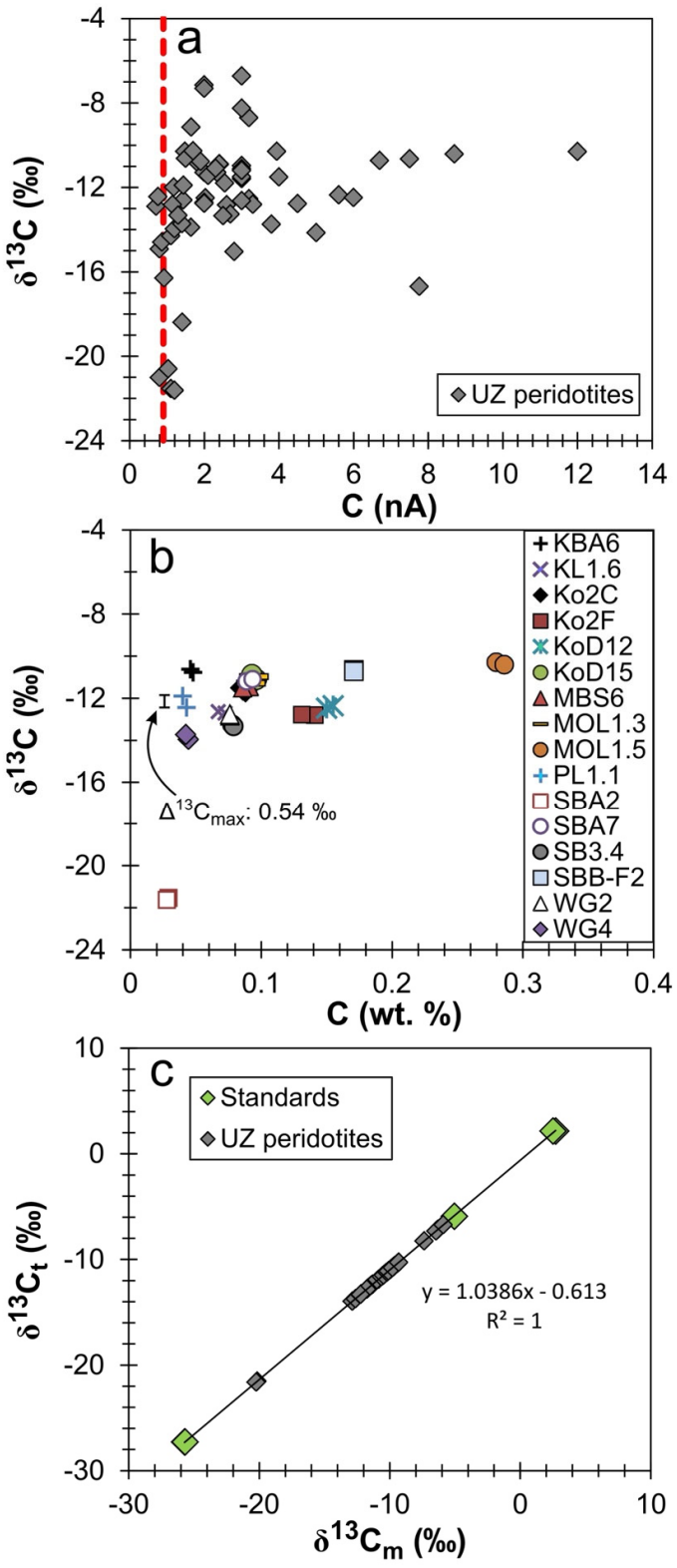

Figure S1 Results of testing the reliability of the analyses for the total carbon content (C) and the carbon isotopic composition ($\delta^{13}C$) in whole-rock peridotites from the Ulten Zone. **a.** Relationship between the obtained signal (nA) and $\delta^{13}C$. The reliability threshold of the signal (stippled line) is 0.9 nA for the peridotites. **b.** Reproducibility of C content and $\delta^{13}C$ for duplicated analyses of the peridotite samples. The maximum variation $\Delta^{13}C$ for duplicates is 0.54‰. **c.** Relationship between the measured isotopic ratio ($\delta^{13}C_m$) and the expected theoretic ratio ($\delta^{13}C_t$) for the three standards defines a interpolation curve. The C isotopic ratios for Ulten Zone peridotites fall on this curve, showing that the sample preparation and analytical approach are suitable for these rocks which have low-carbon matrices.

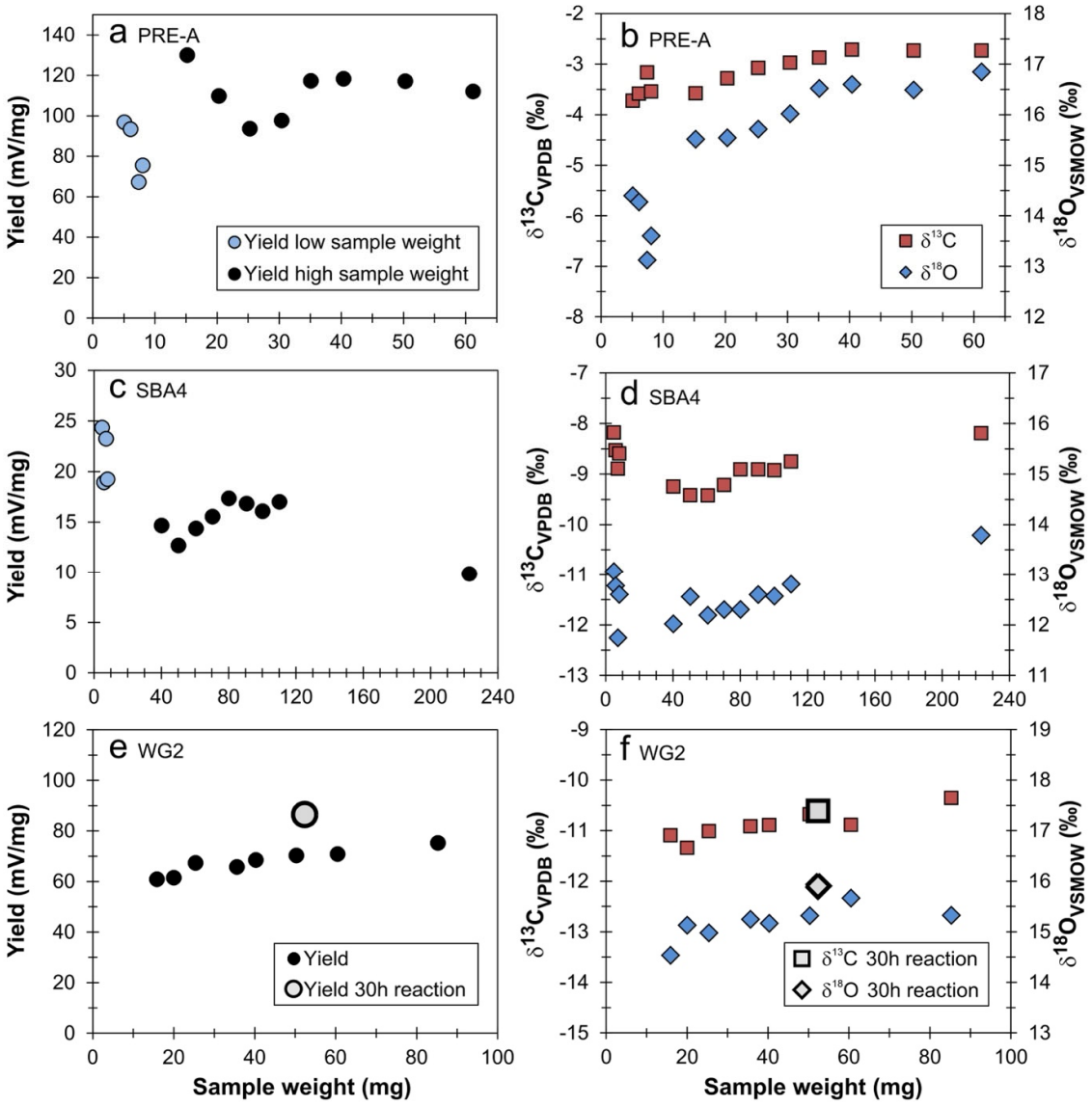

488

489 **Figure S2** Results of testing the required sample amount of Ulten Zone peridotites, which are
490 low-carbonate rocks, for carbonate stable-isotope analyses to obtain reliable results. Tests
491 were carried out on peridotite samples, the carbonate contents of which are known. Variations
492 of **a.** the absolute yield and **b.** $\delta^{13}C$ and $\delta^{18}O$ as a function of the sample weight for sample
493 PRE-A containing calcite veinlets. Different sample amounts were used to check when yield
494 and isotopic compositions remain stable. The same procedure was carried out for samples **c.d.**
495 SBA4 containing dolomite and **e.f.** WG2 containing calcite and dolomite. See Text S1 for
496 detailed explanation.
497

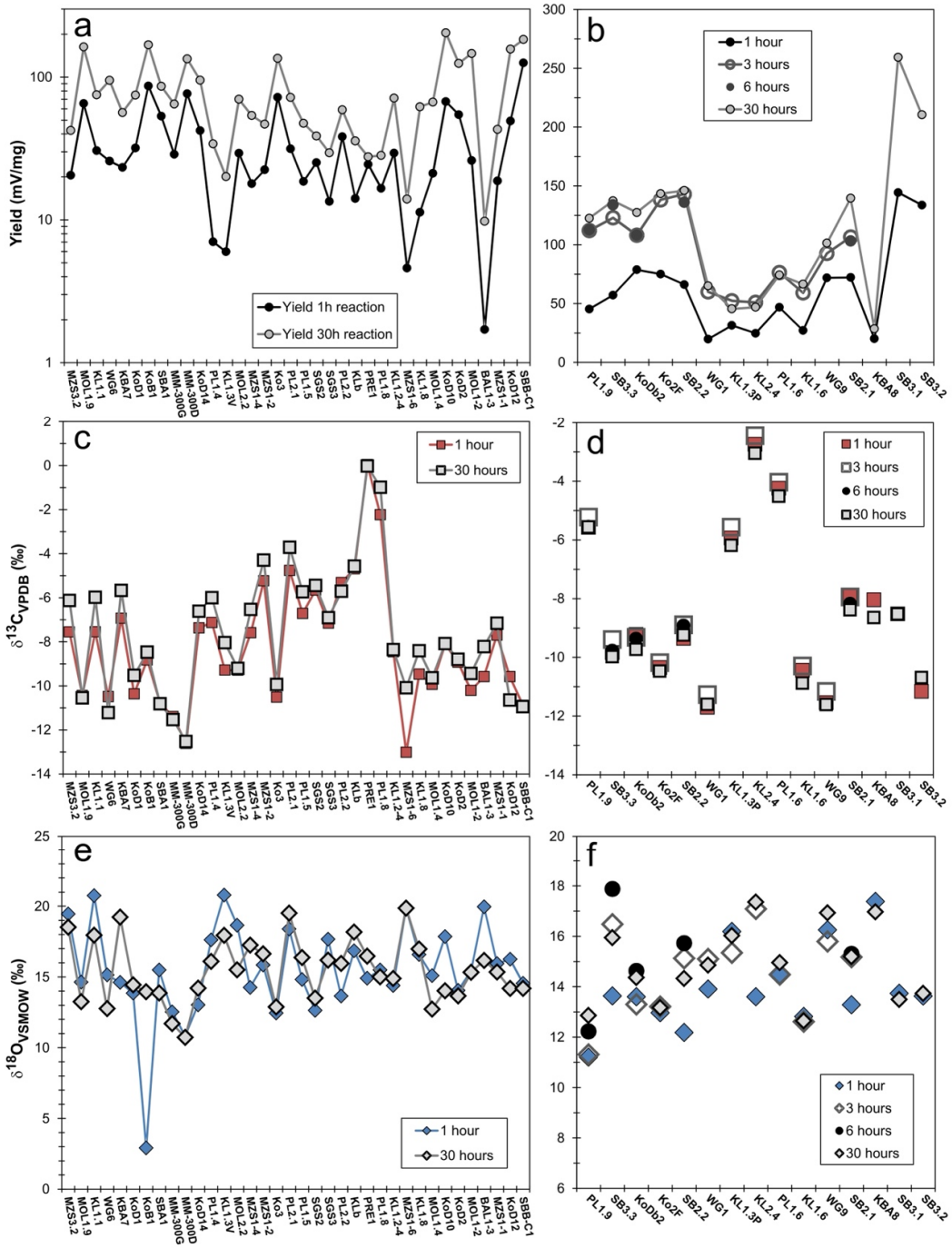

498

499 **Figure S3** Results of testing the required reaction time of carbonates in Ulten Zone
500 peridotites with phosphoric acid in order to obtain reliable results from the carbonate stable-
501 isotope analyses. The highest absolute yield is obtained after 30 hours reaction time for
502 samples with **a.** unknown carbonate content and **b.** most of the samples with multiple
503 carbonate content (calcite-brucite intergrowths ± dolomite). **c.d.** The C isotope ratio ($\delta^{13}C$) for
504 the same samples partly changes significantly after the different reaction times, whereas **e.f.**
505 the O isotopic ratio ($\delta^{18}O$) displays greater variations. Reaction time of 30 hours was accepted
506 as the required reaction time for the carbonate stable-isotope analyses.

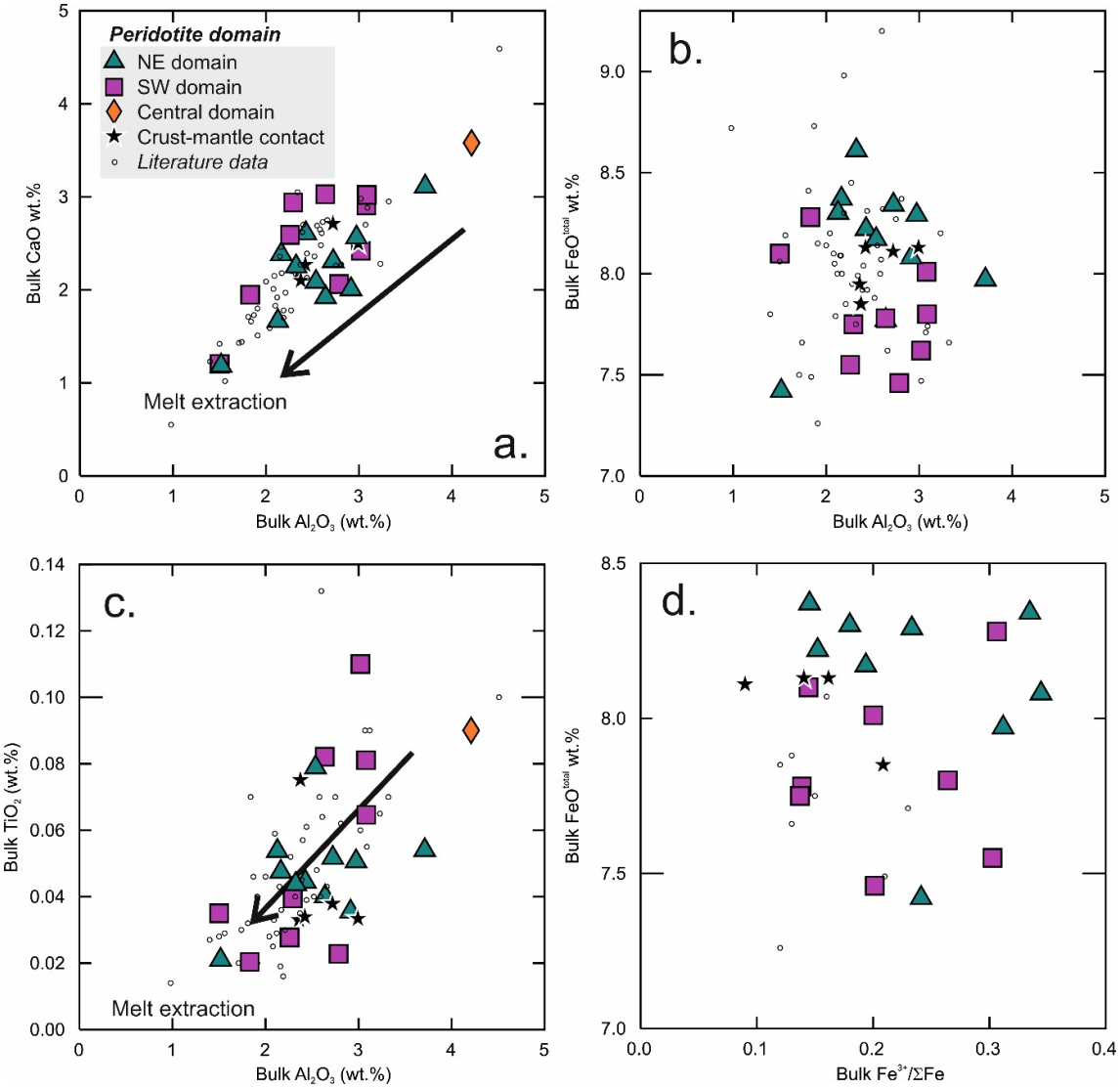

Figure S4 Bulk-rock major-element compositions (wt.%) of Ulten Zone peridotites shown according to domain (Fig. 1a). Al_2O_3 vs. **a.** CaO, **b.** FeO^{total} and **c.** TiO_2, and **d.** $Fe^{3+}/\Sigma Fe$ vs. FeO^{total}. Qualitative melt depletion trends are indicated; literature data are from Marocchi et al. (2009), Ionov et al. (2017), Gudelius et al. (2019) and Consuma et al. (2021).

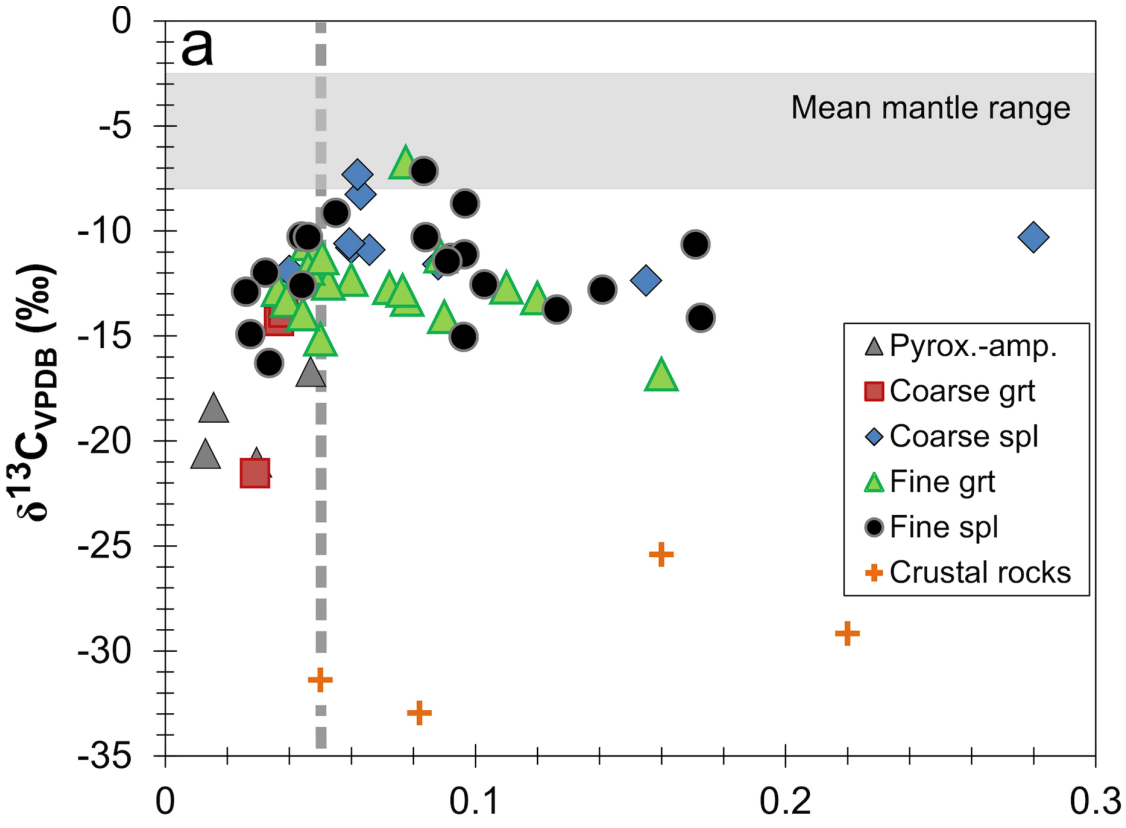

Figure S5 Bulk-rock $\delta^{13}C$ vs. carbon concentration (wt.%). Peridotites are classified by petrographic type regarding the texture (coarse-grained vs. fine-grained) and facies (garnet (grt) vs. spinel (spl)). Pyroxenitic amphibolised samples are not classified as peridotites and shown separately (Pyrox.-amp.). Ulten Zone crustal rocks (gneisses and migmatites) are shown for comparison. The notional mean mantle range for $\delta^{13}C$ is shown for comparison ($\delta^{13}C$ from -8‰ to -2.5‰, Shirey et al., 2013). The dashed line at 0.05 wt. % indicates the C concentration for upper mantle based on 95% of mantle xenoliths (Deines, 2002).

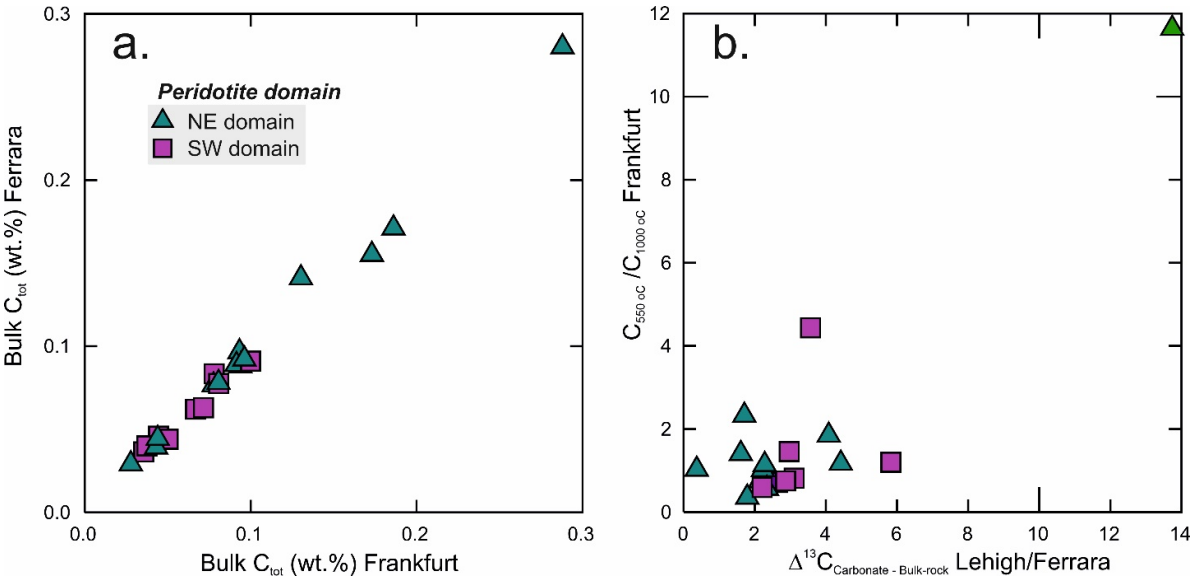

Figure S6 a. Bulk-rock carbon concentration (wt.%) measured in Frankfurt with the LECO multiphase carbon determinator vs. that measured in Ferrara with the Micro Cube Elemental Analyzer (Tables S4 and S5). **b.** Difference between measured carbonate (Lehigh) and bulk-rock $\delta^{13}C$ (Ferrara) vs. the ratio of carbon fractions released at 550 vs. 1000 °C, assumed to be dominated by reduced and organic carbon, respectively.